Analytical and Simulation study for LoRa Modulation

H. Mroue[1,4], A. Nasser[3], B. Parrein[2], S. Hamrioui[1], E. Motta-Cruz[1] and G. Rouyer[4]
[1] IETR UMR CNRS 6164, Université de Nantes, Polytech Nantes, France
[2] LS2N UMR CNRS 6004, Université de Nantes, Polytech Nantes, France
[3] American University of Culture and Education, Beirut, Lebanon
[4] SPIE City Networks, Saint-Herblain, France
Email: hussein.mroue@univ-nantes.fr

Abstract—In this paper, the performance of Long Range (LoRa) Internet of Things (IoT) technology is investigated. By considering Chirp Spread Spectrum (CSS) technique of LoRa, an approximation of the Bit Error Rate (BER) is presented and evaluated through intensive simulations. Unlike previous works which present the BER of LoRa in terms of the ratio of energy ber bit to noise ratio only without any proofing, our presented work expresses BER in terms of LoRa's modulation patterns such as the spreading factor, the code rate, the symbol frequency and the SNR. Numerical results are carried out in order to investigate the LoRa performance and to illustrate the accuracy of the new BER expression.

Index Terms—Internet of Things, LPWAN, LoRa modulation, Chirp Spreading Spectrum (CSS), BER.

I. INTRODUCTION

The Internet of Things (IoT) is a new trend in the development of the wireless communication technologies. Unlike the traditional cellular networks, IoT networks aims at maintaining long range communication with low rate. For this reason, many Low Power Wide Area Network (LPWAN) technologies have recently been emerged in the market. Most of these technologies operate in the Industrial, Scientific, and Medical radio band (ISM band). The spectrum use in ISM band is limited to 1% for uplink and 10% for downlink (duty cycle) [1]. The major advantage of this technology is that the equipment set up is very cheap and consumes a small amount of energy [2]. In the last few years, several technologies have been presented in order to perform LPWAN such as Long Range (LoRa), Sigfox [3], Weightless [4], Narrow-band IoT (NB-IoT) [5], Ingenu RPMA, Telensa, Qowisio, Nwave and Waviot [6], [7]. In this paper, we will focus on LoRa technology, where the LoRa ecosystem architecture is illustrated in Figure 1. The LoRa performance will be investigated by deriving the BER in terms of its proprietary modulation parameters, mainly from end nodes to Gateway.

II. RELATED WORK

In this section, we briefly present recent works on the performance evaluation of LoRa technology [9]–[16]. In [9]–[11], several LPWAN technologies, including LoRa, are compared in terms of coverage range, frequency bands, data rate and capacity. The authors of [12] studied the coverage of LoRa with a channel attenuation mode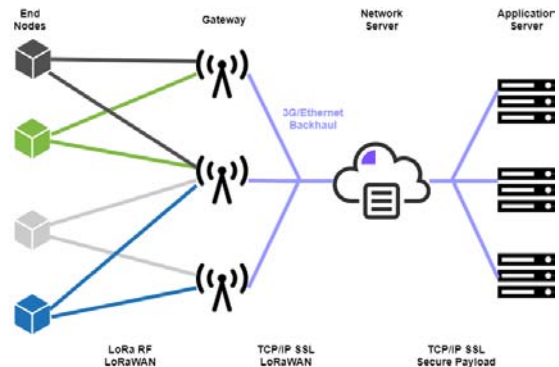l to estimate the required base station density. In [13], the authors analyze the capabilities and limitations of LoRaWAN (Medium Access Control(MAC) layer of LoRa). In [14], the LoRa modulation and demodulation are introduced with the mathematical description and compared to the Frequency Shift Keying (FSK) modulation in terms of BER. In [15], [16], the authors introduce a technical simulation study of an Ultra Narrow Band and CSS protocol for long range communication and a measurement study of their interference sensitivity, and present an estimation of BER expression for CSS without presenting any proofing on the accuracy of their presented expression. Up to our best knowledge, there is no work that has addressed the derivation and the verification of the expression of BER of LoRa.

The major contribution of this paper is to present a performance analysis of LoRa modulation and to validate the results of the analytical BER expression presented in this paper with the experimental ones. In fact, the equation presented in [16] was not verified and it does not show the impact on the BER of several parameters related to the LoRa modulation such as the spreading factor, the symbol frequency, the sampling frequency and the code rate. In this paper, the LoRa performance is investigated in terms of the BER taking into account the physical and the data link layers parameters associated with LoRa modulation. Based on the expression presented in [16], we present an improved expression of the BER showing the spreading effect, the channel coding and the SNR. To validate

Figure 1. LoRa ecosystem architecture

the robustness of this equation, intensive simulations are carried out. These simulations show the good agreement of our BER expression with the numerical results in order to illustrate the effects of SF, the code rate and the SNR on the LoRa performance. Our main goal is to explore all the parameters that affects the BER of CSS used by LoRa modulation.

The rest of this paper is organized as follows. LoRa technology is reviewed in Section II. Analytical and experimental study are explained in Section III. In this section, we describe the analytical expressions and our proposed model to simulate the BER. Finally, the conclusion is given in Section IV.

III. LoRa Physical Layer Introduction

Many existing radio systems use FSK as the physical layer because it is a very efficient modulation at low power. In contrast, LoRa is based on spread spectrum modulation which maintains the similar low power characteristics as FSK. However, LoRa modulation increases the range of communication significantly. The spread spectrum has been used in military and space communication for decades because of the long communication distances that can be achieved and the robustness to interference [17].

A. Chirp Spread Spectrum (CSS) modulation

Chirp stands for 'Compressed High Intensity Radar Pulse', which is a very common technique in sonar and radar. Chirp signals have constant amplitude with a variable frequency. If the frequency changes from lowest to highest, it is called up-chirp and if the frequency changes from highest to lowest, we call it down-chirp. Figure 2 illustrates the LoRa modulation scheme.

CSS can be used to broadcast information on the spectrum. This fact provides resistance to frequency selective noise and jammers at the cost of lower spectral efficiency. Using some extra precautions, CSS may also be more resistant to multipath and Doppler effects than other more conventional modulations such as [18], [19]. In LoRa, the starting frequency of a chirp seems to be used to represent a symbol [21]. The number of encoded bits in a symbol is a tunable parameter, called Spreading Factor (SF). This means that a chirp using the spreading factor SF represents 2^{SF} bits per symbol, meaning that one symbol is represented by multiple chips which are a pulses of a spread spectrum code, such as a Pseudo-Noise (PN) code sequence :

$$SF = \frac{chip\ rate}{symbol\ rate},\qquad(1)$$

CSS implies that the energy of the signal will be spread over a larger band. The spreading factor of a transmission is also used to determine the symbol duration T_s, as follows [22]:

$$T_s = \frac{2^{SF}}{B},\qquad(2)$$

where B denotes the signal bandwidth. Assuming that the modulation uses a fixed bandwidth, an increase in the spreading factor will increase symbol duration. Increasing transmission time for a chirp (Symbol Time) gives the message a greater

robustness to interference or noise. On the other hand, this effect can be partially compensated by the fact that, for higher spreading factors, the number of symbols increases, which makes the frequency of symbol errors bigger, where the synchronisation between the receiver and the signals is particularly critical when small data bits are used. Another disadvantage of longer message transmission is the higher probability of collisions. Indeed, SF affects the sensitivity S of the receiver that is defined as [22]:

$$S = -174 + 10\log_{10}(B) + NF + SNR,\qquad(3)$$

where (-174) is due to the thermal noise at the receiver in 1 Hz bandwidth, NF is the Noise Figure at the receiver (which is fixed for a hardware configuration data) and SNR is the signal to noise ratio required for the modulation. According to [22], the binary data rate R_b can be expressed as follows :

$$R_b = SF \times \frac{B}{2^{SF}}.\qquad(4)$$

Table I illustrates LoRa bit rates, symbol durations and sensitivity as regards to the spreading factor.

Table I
LoRa bit rates, symbol durations and sensitivity *vs* SF

Mode	Bit rate (b/s)	Symbol duration (ms)	Sensitivity (dBm)
LoRa SF 12	293	682	-137
LoRa SF 11	537	365	-134.5
LoRa SF 10	976	204	-132
LoRa SF 9	1757	113	-129
LoRa SF 8	3125	64	-126
LoRa SF 7	5468	36	-123
LoRa SF 6	9375	21	-118
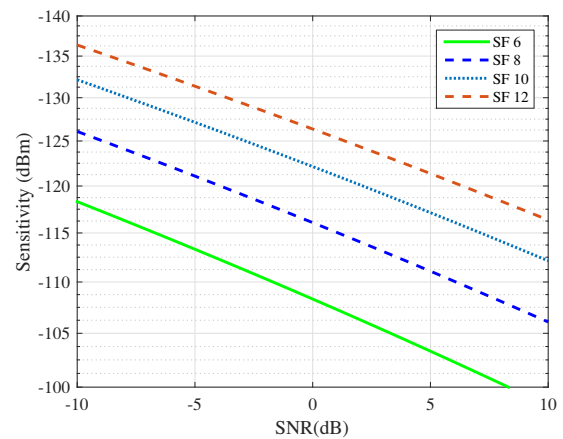
Figure 3. Spread spectrum vs the Sensitivity of LoRa receiver

Figure 3 shows the sensitivity of LoRa receiver as a function of SNR. The sensitivity is calculated according to (3). Figure 3 also shows that the sensitivity of LoRa receiver is affected by the increase of the spreading factor: when the spreading factor increases the sensitivity increases which implies that the receiver can retrieve data despite a low level of SNR. It is recommended to use a high SF to be able to retrieve the signal correctly.

Figure 2. LoRa modulation scheme

B. Decoding LoRa frame

LoRa is based on the modulation of the spectrum with the same low-power characteristics of the FSK modulation, but it considerably increases the coverage range. In addition to the modulation itself, LoRa also specifies a set of encoding values that are applied before modulation and transmission. The decoding stages are as follows [21]:

1) Forward Error Correction (FEC): LoRa uses Hamming codes for Forward Error Correction (FEC). This is a simple linear block code algorithm which is easy to implement. The length of the code information word is set to 4 bits and the length of the code word is a tunable parameter in the range (5-8) bits. LoRa offers Code Rates (CR) of 4/5, 4/6, 4/7 and 4/8. If the code blocks are defined such that the minimum hamming distance is 1, 2, 3 and 4 for code rates 4/5, 4/6, 4/7 and 4/8 respectively, the error correction and error detection capabilities are as shown in Table II [20].

Table II
ERROR CORRECTION AND DETECTION CAPABILITIES OF LoRa

Code Rate	Error Correction (bits)	Error detection (bits)
4/5	0	0
4/6	0	1
4/7	1	2
4/8	1	3

As shown in Table II, error correcting is only introduced by the 4/7 code rate. Furthermore, code rate 4/8 does not improve error correction capabilities but only detection capabilities. Code rate 4/5 offers no clear advantage over no coding, and code rate 4/6 only increase the number of detected wrong bits, but no correction is enhanced. Therefore, in order to have actual error correcting capabilities, at least code rate 4/7 must be used. However, introducing coding and utilizing code rate 4/7 increases the payload length by 75% compared to no coding.

2) Data whitening: In order to provide more features for clock recovery by the receiver, data whitening is applied to induce randomness into the symbols. Data whitening also helps to distribute information over the entire bandwidth of the radio channel. The received symbols may be de-whitened by XORing them with the same whitening sequence used by the transmitter.

3) Interleaving: Interleaving is a technique that scrambles data bits throughout the packet. It is combined with FEC to make the data more robust to interference. LoRa implements a diagonal interleaver, with the most significant two bits reversed. Each diagonal word is offset, or rotated, by an arbitrary number of bits. Finally, the bits within each codeword are reversed.

4) Gray Indexing: Gray Indexing is finally used to map a block of SF bits in M symbols in the constellation, while ensuring that two adjacent symbols differ by no more than 1 bit, to increase the chances of the channel code and correct possible errors.

LoRa uses a variable error correction scheme that improves the robustness of transmitted signal. The data rate expressed by (4) is now modified as follows [22]:

$$R_b = SF \times \frac{B}{2^{SF}} \times \frac{4}{4 + CR} \qquad (5)$$

CR is the code rate, where $CR \in \{1, 2, 3, 4\}$.

C. Orthogonality of the Spreading Factors

A very powerful feature of the LoRa modulation is that the SFs are pseudo-orthogonal. This allows a receiver to properly detect a packet using the spreading factor i even if it overlaps in time with another transmission using a spreading factor j, as long as $i \neq j$ and the Signal to Interference plus Noise ratio (SINR) of the packet received is greater than a certain threshold which depends on both i and j. This pseudo-orthogonality between different packets allows a network using LoRa devices to exploit different SFs to reach a higher rate of flow compared to more traditional modulation schemes, in which a collision

can cause an incorrect reception of the expected packet and the jammer.

IV. ANALYTICAL AND SIMULATION STUDY

In this section the analytical and simulation results are presented. First, the model validation results are introduced, after which the simulation results are discussed.

A. Analytical Study

According to [16], the estimation of the analytical expression for the error probability of CSS ($P_{e,CSS}$) is given by:

$$P_{e,CSS} = Q\left(\frac{\log_{12}(SF)}{\sqrt{2}} \frac{E_b}{N_0}\right), \quad (6)$$

where $Q(.)$ and $\frac{E_b}{N_0}$ denote respectively the Q-function and the energy per bit to noise power spectral density ratio.

This equation shows that for higher SF, the BER is more acute. The use of $\frac{E_b}{N_0}$ does not reflect the perfect case, because in CSS the energy is spread over a large band and depends on several parameters that vary from one system to another. Our problem is related to the conversion from $\frac{E_c}{N_0}$ to $\frac{E_b}{N_0}$. Where $\frac{E_c}{N_0}$ is the energy per chip-time to noise power spectral density ratio. According to [23], $\frac{E_c}{N_0}$ is given by:

$$\frac{E_c}{N_0} = \frac{E_b}{N_0} + 10\log_{10}\left(\frac{R_c M_0}{SF}\right) + L, \quad (7)$$

where R_c, M_0, SF and L denote the code rate of the FEC, the modulation order in bits/sym (note that $M_0 = 1$ for all spread spectrum applications), the spreading factor and the additional implementation loss, respectively.

We notice that in CSS, the chip represents the symbol multiplied by SF (equation (1)), therefore the energy per chip is equal to the energy per symbol multiplied by SF ($\frac{E_c}{N_0} = \frac{E_s}{N_0} \times SF$), where $\frac{E_s}{N_0}$ denotes the energy per symbol). Analytical expression of $\frac{E_s}{N_0}$ is given by:

$$\frac{E_s}{N_0} = 10\log_{10}\left(\frac{f_{sym}}{f_{samp}}\right) + SNR \quad (8)$$

where f_{sym}, f_{samp} and SNR denote the symbol frequency, the sampling frequency and the signal-to-noise ratio, respectively. Therefore,

$$\frac{E_c}{N_0} = \frac{E_s}{N_0} \times SF \\ = \left[10\log_{10}\left(\frac{f_{sym}}{f_{samp}}\right) + SNR\right] \times SF, \quad (9)$$

Thanks to (7) and (9), we obtain (10).

$$\frac{E_b}{N_0} = \left[10\log_{10}\left(\frac{f_{sym}}{f_{samp}}\right) + SNR\right] \times SF \\ - 10\log_{10}\left(\frac{R_c M_0}{SF}\right) - L, \quad (10)$$

Thanks to (6) and (10), we obtain (11).

Table III
SIMULATION PARAMETERS

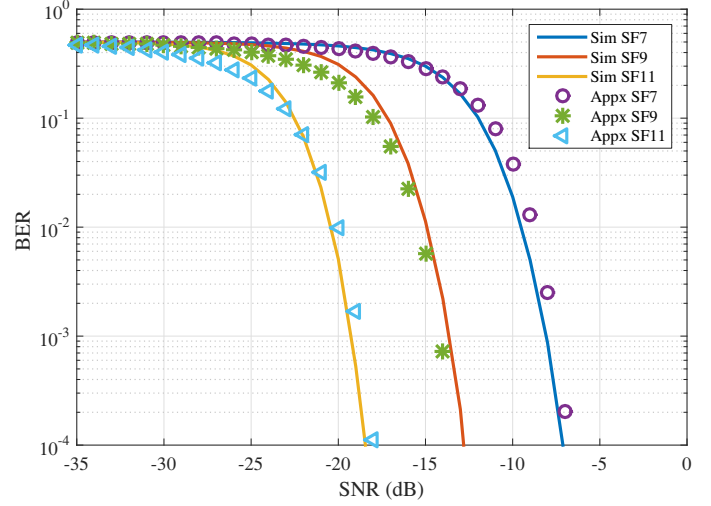| Code Rate	4/8
SF	7-9-11
Packet size	243 bytes
Bandwidth	125 KHz
f_{samp}	125 KHz
SNR [dB]	[-35:0]

Figure 4. Approximation and simulation BER for LoRa transmissions

$$P_{e,CSS} = Q\left(\frac{\log_{12}(SF)}{\sqrt{2}} \times \left[10\log_{10}\left(\frac{f_{sym}}{f_{samp}}\right) + SNR\right] \\ \times SF - 10\log_{10}\left(\frac{R_c M_0}{SF}\right) - L\right). \quad (11)$$

Finally, $P_{e,CSS}$ is given by (11). Unlike (6) proposed in [16], $P_{e,CSS}$ has a non linear form. (11) shows that $P_{e,CSS}$ depends on f_{sym}, f_{samp}, R_c, SF, L and SNR. The use of these parameters is more accurate, due to the fact that these parameters are not linearly dependent on $\frac{E_b}{N_0}$ (i.e. symbol frequency, sampling frequency and implementation loss vary from one system to another).

B. Simulation Study and Results

To validate our proposal, the BER of LoRa transmission was simulated using 3 spreading factors with a 200 rounds Monte-Carlo. AWGN (Additive White Gaussian Noise) channel is considered in the model. All the parameters of the simulation are given in Table III. We consider the uplink in the simulation because the data in sensor networks generally flows in uplink way. The data are modeled as packets of 243 bytes (the maximum payload length to be transmitted in LoRa message [24]).

Figure 4 shows the analytical and experimental results of the BER for LoRa transmissions using 3 spreading factors 7, 9 and
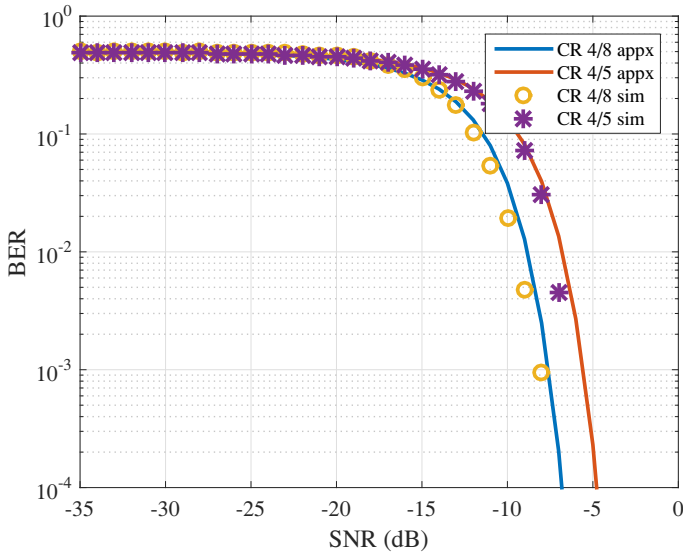
Figure 5. Approximation and simulation BER for LoRa with $SF = 7$, $CR = \frac{4}{5}, \frac{4}{8}$.

11. Figure 4 also shows that the simulation results fit with the analytical ones, and thus validates our model. The results of the simulation are compatible with (11) because when SF increases, the $P_{e,CSS}$ decreases. As expected, the BER decreases with the SF, at $SNR = -15 \; dB$ the BER is about 5.10^{-2} when using $SF = 11$, whereas, the BER becomes $10^{-0.8}$ when using $SF = 7$.

Figure 5 shows the analytical and experimental results of the BER for LoRa SF 7 using 2 different coding rates ($CR = \frac{4}{5}, \frac{4}{8}$). The simulation results are with good agreement with approximation ones for the two considered value of code rates. As expected, the BER decreases with the code rate, at $SNR = -10dB$, the BER is about 2.10^{-2} when using $CR = \frac{4}{8}$, whereas, the BER becomes $1,5.10^{-1}$ when using $CR = \frac{4}{5}$. Thus, it is advised to adopt a low CR in order to decrease as possible the BER. In contrast, a low CR may negatively impact the throughput rate of the LoRa system.

V. Conclusion

In this paper, the physical layer of the IoT communication standard LoRa is studied. Approximation expression of the Bit Error Rate (BER) of LoRa is presented and validated by numerical results. This expression is related to the physical and Data link layer parameters (spreading factor, coding rate, symbol frequency and sampling frequency) unlike the existing works where the BER was a function of energy per bit to noise power spectral density ratio ($\frac{E_b}{N_0}$). Numerical results show that for a wide range variation of SNR and different values of the spreading factor and the code rate, this approximation kept accurate results.

VI. Acknowledgement

References

[1] ETSI EN 300 220-1, V3.1.0, "Short Range Devices (SRD) operating in the frequency range 25 MHz to 1000 MHz; Part 1: Technical characteristics and methods of measurement", 2016.

[2] J. Petäjäjärvi, K. Mikhaylov, M. Hämäläinen and J. Iinatti, "Evaluation of LoRa LPWAN technology for remote health and wellbeing monitoring," 2016 10th International Symposium on Medical Information and Communication Technology (ISMICT), Worcester, MA, 2016.

[3] M. Centenaro, L. Vangelista, A. Zanella and M. Zorzi, "Long-range communications in unlicensed bands: the rising stars in the IoT and smart city scenarios," in IEEE Wireless Communications, October 2016.

[4] Weightless. [Online]. Available: http://www.weightless.org/

[5] A. Hoglund et al., "Overview of 3GPP Release 14 Enhanced NB-IoT," in IEEE Network, vol. 31, no. 6, pp. 16-22, November/December 2017.

[6] U. Raza, P. Kulkarni and M. Sooriyabandara, "Low Power Wide Area Networks: An Overview," in IEEE Communications Surveys and Tutorials, vol. 19, no. 2, pp. 855-873, Q2 2017.

[7] B. Moyer, "Low Power, Wide Area : A Survey of Longer-Range IoT Wireless protocols", Electronic Engineering Journal, 2015. [Online] Available: http://www.eejournal.com/article/20150907-lpwa/telecommunications.html

[8] N. Sorin, M. Luis, T. Eirich, T. Kramp and O. Hersent, "LoRaWAN Specification," LoRa Alliance Inc., San Ramon, CA, Version. 1.0; 2015.

[9] N. Rathod et al., "Performance analysis of wireless devices for a campus-wide IoT network," 2015 13th International Symposium on Modeling and Optimization in Mobile, Ad Hoc, and Wireless Networks (WiOpt), Mumbai, 2015, pp. 84-89.

[10] M. Centenaro, L. Vangelista, A. Zanella and M. Zorzi, "Long-range communications in unlicensed bands: the rising stars in the IoT and smart city scenarios," in IEEE Wireless Communications, vol. 23, no. 5, pp. 60-67, October 2016.

[11] B. Vejlgaard, M. Lauridsen, H. Nguyen, I. Z. Kovacs, P. Mogensen and M. Sorensen, "Coverage and Capacity Analysis of Sigfox, LoRa, GPRS, and NB-IoT," 2017 IEEE 85th Vehicular Technology Conference (VTC Spring), Sydney, NSW, 2017, pp. 1-5.

[12] J. Petajajarvi, K. Mikhaylov, A. Roivainen, T. Hanninen and M. Pettissalo, "On the coverage of LPWANs: range evaluation and channel attenuation model for LoRa technology," 2015 14th International Conference on ITS Telecommunications (ITST), Copenhagen, 2015.

[13] F. Adelantado, X. Vilajosana, P. Tuset-Peiro, B. Martinez, J. Melia-Segui and T. Watteyne, "Understanding the Limits of LoRaWAN," in IEEE Communications Magazine, vol. 55, no. 9, pp. 34-40, 2017.

[14] L. Vangelista, "Frequency Shift Chirp Modulation: The LoRa Modulation," in IEEE Signal Processing Letters, Dec. 2017.

[15] B. Reynders and S. Pollin, "Chirp spread spectrum as a modulation technique for long range communication," 2016 Symposium on Communications and Vehicular Technologies (SCVT), Mons, 2016, pp. 1-5.

[16] B. Reynders, W. Meert and S. Pollin, "Range and coexistence analysis of long range unlicensed communication," 2016 23rd International Conference on Telecommunications (ICT), Thessaloniki, 2016.

[17] R. L. Pickholtz, L. B. Milstein and D. L. Schilling, "Spread spectrum for mobile communications," in IEEE Transactions on Vehicular Technology, vol. 40, no. 2, pp. 313-322, May 1991.

[18] M. Kowatsch and J. Lafferl, "A spread-spectrum concept combining chirp modulation and pseudonoise coding," IEEE Transactions on Communications, vol. 31, no. 10, pp. 1133– 1142, Oct 1983.

[19] A. Springer, W. Gugler, M. Huemer, R. Koller, and R. Weigel, "A wireless spread-spectrum communication system using saw chirped delay lines," IEEE Transactions on Microwave Theory and Techniques, vol. 49, no. 4, pp. 754–760, Apr 2001.

[20] A. G. i Amat, "SSY125 Digital Communications, Lecture Notes," Department of Signals and Systems, Chalmers University of Technology, Nov. 2015.

[21] M. Knight and B. Seeber, "Decoding LoRa: Realizing a Modern LPWAN with SDR," 6th GNU Radio Conference, 2016.

[22] Semtech, "LoRa Modulations basics", AN 1200.22, May 2015.

[23] Comtechefdata, "Spread Spectrum in the SLM-5650A: Features, Performance, and Applications," Oct 2012.

[24] Ka. Mekki, E. Bajic, F. Chaxel and F. Meyer, "A comparative study of LPWAN technologies for large-scale IoT deployment," ICT Express, 2018, ISSN 2405-9595.